

Synthesis, structure and dielectric properties of new oxide compounds $\text{Ln}_{1-x}\text{Sr}_{1+x}\text{Cu}_{x/2}\text{Ti}_{1-x/2}\text{O}_4$ ($\text{Ln} = \text{La, Pr, Nd}$) belonging to the structural type of K_2NiF_4

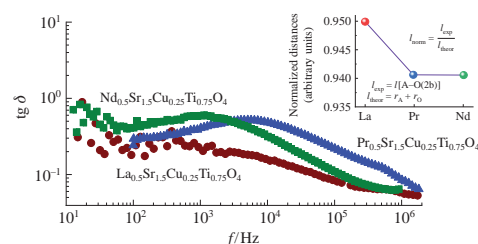
Tatyana I. Chupakhina,^a Yulia A. Deeva,^{*a,b} Nina V. Melnikova,^b Vladimir V. Gorin,^b Ilya S. Sivkov^b and Olga I. Gyrdasova^a

^a Institute of Solid State Chemistry, Ural Branch of the Russian Academy of Sciences, 620990 Ekaterinburg, Russian Federation. Fax: +7 343 374 4495; e-mail: juliahik@mail.ru

^b Ural Federal University, 620002 Ekaterinburg, Russian Federation

DOI: 10.1016/j.mencom.2019.05.037

New complex oxides $\text{Ln}_{1-x}\text{Sr}_{1+x}\text{Cu}_{x/2}\text{Ti}_{1-x/2}\text{O}_4$ (where Ln is La, Pr, or Nd) possessing the K_2NiF_4 type structure were synthesized. Their structure and dielectric properties were characterized. Low values of the dielectric loss tangent in the radio frequency range have been revealed, which correlates with their structural anisotropy and morphology.



Complex oxides of the general formula A_2BO_4 possessing a K_2NiF_4 type structure exhibit a variety of electrical and magnetic properties allowing them to be employed in a number of practical applications. Since the majority of these oxides contain elements with variable valency and possess a high electrical conductivity, their transport properties are widely investigated. Some oxides [$\text{La}_2\text{CuO}_{4+\delta}$, $\text{Ln}_{2-x}\text{Sr}_x\text{NiO}_4$ (Ln is La, Pr, or Nd) and $\text{La}_{2-x}\text{Sr}_x\text{Ni}_{1-y}\text{M}_y\text{O}_4$ (M = Mg, Al)]^{1–3} with a K_2NiF_4 type of structure demonstrate a giant dielectric permeability. Considerable attention is also paid to solid solutions $\text{La}_{2-x}\text{Sr}_x\text{Ni}_{1-y}\text{M}_y\text{O}_4$, since large dielectric constant values in single crystals and ceramic samples obtained on their basis are preserved in a wide range of frequencies and temperatures. Nevertheless, due to the high through conductivity caused by the variable valency of transition metals, there are high dielectric losses in the most of materials studied.

The reasons for the high dielectric permittivity observed in perovskite-like oxides that are not ferroelectrics are still not understood and remain of interest including the case of materials possessing the K_2NiF_4 type structure.^{1–5} As the possible reasons for the high dielectric constant, a distortion of coordination polyhedra, a charge polarization, and a polaron mechanism of conductivity were proposed. It is also assumed that the dielectric loss angle tangent ($\text{tg}\delta$) in the oxides with the K_2NiF_4 type structure decreases upon a replacement of the lanthanides with alkaline earth metals.² At this end, it seems relevant to look for new composite materials having high dielectric permittivity and a smaller value of the dielectric loss tangent among the compounds with the K_2NiF_4 type structure.

This work was aimed at the synthesis of new series of solid solutions $\text{Ln}_{1-x}\text{Sr}_{1+x}\text{Cu}_{x/2}\text{Ti}_{1-x/2}\text{O}_4$ (Ln = La, Pr, Nd) based on complex oxides possessing the K_2NiF_4 type structure, their characterization by impedance spectroscopy and X-ray diffraction methods, and evaluation as potential materials for practical applications in electronic devices.

The structural characteristics and magnetic properties of $\text{La}_{2-x}\text{Sr}_x\text{Ti}_{1-y}\text{Cu}_y\text{O}_4$ solid solutions have already been reported,⁶ special attention being paid the studies of compounds with $y = 0.5$. However, the solid solutions with $x(\text{La}) > 0.65$ are not single-phase ones. It is known that the elementary cell of complex oxides of the general formula A_2BO_4 (where A are lanthanides and/or alkaline earth metals and B are usually occupied by *d*-metals) can be represented as coordination polyhedra of AO_9 combination (one-cap tetragonal antiprism) and octahedra BO_6 . Isomorphous substitution in antiprisms and octahedra in the case of Sr_2TiO_4 – La_2CuO_4 system can be carried out either at the strontium titanate or lanthanum cuprate parts. However, the $\text{La}_{1.7}\text{Sr}_{0.3}\text{Ti}_{0.85}\text{Cu}_{0.15}\text{O}_4$ sample was reported⁶ as already containing impurity phases, while $\text{Sr}_{2-x}\text{La}_x\text{Ti}_{1-y}\text{Cu}_y\text{O}_4$ solid solutions have a wider homogeneity range.

The general formula of solid solutions with conjugated heterovalent substitution at A and B positions with oxygen stoichiometry preservation can be represented as $\text{Ln}_{1-x}\text{Sr}_{1+x}\text{Cu}_{x/2}\text{Ti}_{1-x/2}\text{O}_4$. We have synthesized samples, where the value x was 0.5 (Ln = La, Pr, Nd).[†] Figure 1 shows the micrographs of these samples

[†] The reported oxides were synthesized according to the standard ceramic technology using the oxides and carbonates of the corresponding metals as the starting reagents. The powder obtained after grinding and pretreating at 970 °C was pressed at $P = 200$ bar and annealed at 1050, 1100 and 1150 °C for 8 h. Note that the phase formation process was fully completed at 1100 °C for all the samples, and they did not contain any impurities. However, this temperature does not provide the production of gas-tight ceramics. Temperature increase to 1150 °C allowed us to obtain gas-tight ceramics of the compositions $\text{La}_{0.5}\text{Sr}_{1.5}\text{Cu}_{0.25}\text{Ti}_{0.75}\text{O}_4$ and $\text{Nd}_{0.5}\text{Sr}_{1.5}\text{Cu}_{0.25}\text{Ti}_{0.75}\text{O}_4$, however the sample $\text{Pr}_{0.5}\text{Sr}_{1.5}\text{Cu}_{0.25}\text{Ti}_{0.75}\text{O}_4$ had still contained main pores. X-ray phase analysis data on samples processed at 1200 °C indicated phase stability of solid solutions containing lanthanum and neodymium, whereas CuO and SrO were present in the diffractogram of $\text{Pr}_{0.5}\text{Sr}_{1.5}\text{Cu}_{0.25}\text{Ti}_{0.75}\text{O}_4$. To compare the properties of all the three oxides obtained under the same conditions, ceramic samples sintered at 1150 °C were used.

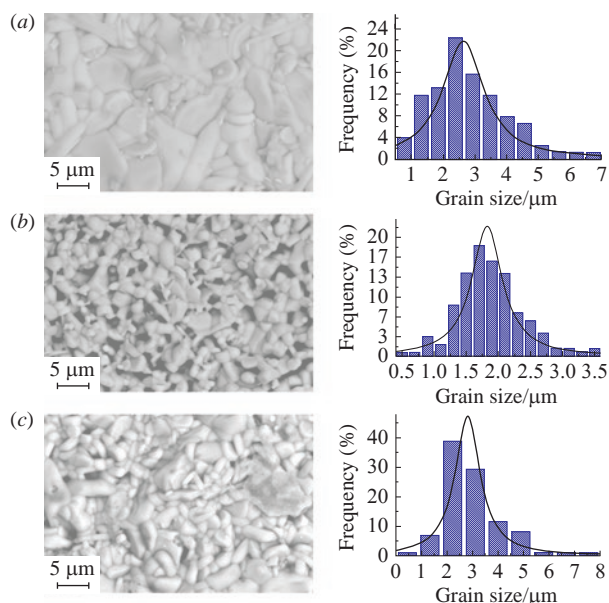


Figure 1 SEM images of the surface of obtained $\text{Ln}_{0.5}\text{Sr}_{1.5}\text{Cu}_{0.25}\text{Ti}_{0.75}\text{O}_4$ samples: (a) Ln = Nd, (b) Ln = Pr, (c) Ln = La. The right parts show the respective grain size distribution for each sample.

obtained at 1150 °C and the particle size distribution. One can see that despite processing under the same conditions, the sample surface morphology depends strongly on the type of the replacement element. The morphological samples $\text{Ln}_{0.5}\text{Sr}_{1.5}\text{Cu}_{0.25}\text{Ti}_{0.75}\text{O}_4$ (Ln = La, Pr, Nd) performed in the BES (back-reflected electron) survey mode indicate a single-phase nature of the compounds obtained, based on the monochrome X-ray contrast distribution.

Sample $\text{Nd}_{0.5}\text{Sr}_{1.5}\text{Cu}_{0.25}\text{Ti}_{0.75}\text{O}_4$ [Figure 1(a)] consists of close-packed round-shaped crystallites, whose size distribution is non-uniform. Large particles (4–7 μm) are surrounded by smaller ones (0.1–3 μm). The particles densely adjoin together, which is typical of the gas-dense ceramics.

Ceramics $\text{Pr}_{0.5}\text{Sr}_{1.5}\text{Cu}_{0.25}\text{Ti}_{0.75}\text{O}_4$ [Figure 1(b)] is formed of poorly crystallized particles sized in the range from 0.6 to 3.5 μm. A significant number of main pores should be noted, and their average size is ~2 μm.

Sample $\text{La}_{0.5}\text{Sr}_{1.5}\text{Cu}_{0.25}\text{Ti}_{0.75}\text{O}_4$ [Figure 1(c)] represents almost the same number of crystalline structures (the majority of particles have a size of 2–4 μm) adjacent tightly to each other. The pores are present in small quantities.

The average cationic composition of La: Sr: Cu: Ti was confirmed by EDX analysis and without taking into account the C content in the carbon adhesive tape, was 2:6:1:3 within the experimental error.

Figure 2 shows the experimental, theoretical and difference diffractograms of compound $\text{Pr}_{1-x}\text{Sr}_{1+x}\text{Cu}_{x/2}\text{Ti}_{1-x/2}\text{O}_4$.[‡] The diffractograms of $\text{La}_{1-x}\text{Sr}_{1+x}\text{Cu}_{x/2}\text{Ti}_{1-x/2}\text{O}_4$ and $\text{Nd}_{1-x}\text{Sr}_{1+x}\text{Cu}_{x/2}\text{Ti}_{1-x/2}\text{O}_4$ demonstrated a similar profile. All samples were single-phase ones without any reflexes of impurities. The crystal-chemical parameters of $\text{Ln}_{0.5}\text{Sr}_{1.5}\text{Cu}_{0.25}\text{Ti}_{0.75}\text{O}_4$ are summarized in Table 1.

Figure 3 shows the frequency dependences of the permittivity and dielectric loss tangent for compound $\text{Ln}_{0.5}\text{Sr}_{1.5}\text{Cu}_{0.25}\text{Ti}_{0.75}\text{O}_4$. The dielectric constant of the samples was $\sim 10^2$ [see Figure 3(a)], and the loss tangent values for all the compounds were close to each other being of the order of 1 or less. It was found that the smallest value of $\text{tg}\delta$ belongs to compound $\text{La}_{0.5}\text{Sr}_{1.5}\text{Cu}_{0.25}\text{Ti}_{0.75}\text{O}_4$,

Table 1 Crystal structure parameters for $\text{Ln}_{0.5}\text{Sr}_{1.5}\text{Cu}_{0.25}\text{Ti}_{0.75}\text{O}_4$ solid state solutions [space group $I4/mmm$ (#139), Cu/Ti fraction 0.25/0.75 (2a) 0, 0, 0; Ln/Sr fraction 0.33/0.67 (4e) 0, 0, z; O(1)(4c) 0.5, 0, 0 and O(2)(4e) 0, 0, z].

Parameter	Atom		
	La	Pr	Nd
$a = b/\text{Å}$	3.8641 ± 0.0002	3.8538 ± 0.0001	3.8484 ± 0.0002
$c/\text{Å}$	12.7703 ± 0.0008	12.7169 ± 0.0004	12.6907 ± 0.0009
$V/\text{Å}^3$	190.672 ± 0.018	188.868 ± 0.009	187.918 ± 0.002
$z(\text{Ln/Sr})$	0.3557 ± 0.0013	0.3560 ± 0.0010	0.35580 ± 0.0023
$z(\text{O}_2)$	0.3557 ± 0.0013	0.1656 ± 0.0006	0.1649 ± 0.0003
R_p	5.38	4.14	5.44
R_{wp}	8.29	6.19	7.94
R_B	3.87	3.39	3.21
R_f	4.13	3.22	3.76
χ^2	1.422	0.948	1.056
Overall B-factor	0.4553	0.3974	0.4458
Interatomic distances/Å			
Cu–O(1)(x4)	1.930 ± 0.002	1.927 ± 0.001	1.924 ± 0.001
Cu–O(2)(x2)	2.057 ± 0.002	2.105 ± 0.008	2.096 ± 0.002
Ln–O(1)(x4)	2.670 ± 0.002	2.658 ± 0.001	2.655 ± 0.001
Ln–O(2a)(x4)	2.741 ± 0.001	2.739 ± 0.001	2.736 ± 0.001
Ln–O(2b)(x1)	2.485 ± 0.003	2.423 ± 0.002	2.427 ± 0.009

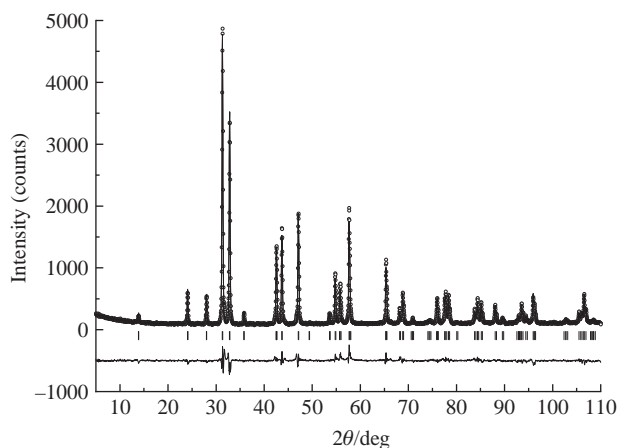


Figure 2 The theoretical, experimental and difference diffractograms of compound $\text{Pr}_{1-x}\text{Sr}_{1+x}\text{Cu}_{x/2}\text{Ti}_{1-x/2}\text{O}_4$.

while the largest ϵ value is characteristic of $\text{Pr}_{0.5}\text{Sr}_{1.5}\text{Cu}_{0.25}\text{Ti}_{0.75}\text{O}_4$ [see Figure 3(b)]. The latter value may be related to the microstructure of the sample. In ceramic materials, the apparent value of the dielectric constant is significantly affected by processes associated with charge transfer inside the grains near their boundaries, as well as at the boundaries of inhomogeneities. An increase in the total area of grain boundaries in a unit volume of a non-gas-tight sample $\text{Pr}_{0.5}\text{Sr}_{1.5}\text{Cu}_{0.25}\text{Ti}_{0.75}\text{O}_4$ as compared to the other two materials, whose microstructure is characterized by the presence of close-packed crystallites, and the Maxwell–Wagner effect in the investigated materials could lead to higher values of the measured dielectric constant. However, these dielectric constants are not as high as it might be expected in comparison with those of the other two gas-tight samples. Consequently, there were other reasons for the higher dielectric constant values in the case of $\text{Pr}_{0.5}\text{Sr}_{1.5}\text{Cu}_{0.25}\text{Ti}_{0.75}\text{O}_4$.

Analysis of the structural parameters revealed that the greatest distortion of the coordination polyhedra of the unit cell occurs in compound $\text{Pr}_{0.5}\text{Sr}_{1.5}\text{Cu}_{0.25}\text{Ti}_{0.75}\text{O}_4$. There is a hypothesis that in oxides possessing the K_2NiF_4 structure, the dielectric properties correlate with anisotropy of the antiprism of AO_9 and octahedra BO_6 , which represent the coordination polyhedra of the unit cell.^{7,8} There is a relationship between the increase in the

[‡] X-ray phase and X-ray diffraction analyses were performed using a Shimadzu XRD-7000 S automatic diffractometer with exposure for 3–5 s in point. The resulting diffractograms were processed by the Rietveld method using the Fullprof 2016 software.

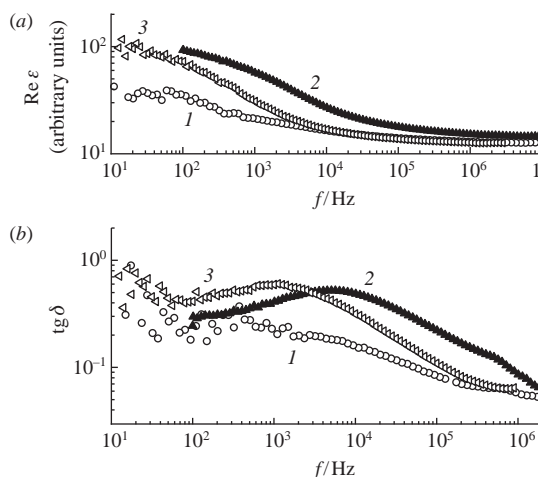


Figure 3 Frequency dependences of (a) the dielectric permittivity and (b) the dielectric loss tangent for compounds $\text{Ln}_{0.5}\text{Sr}_{1.5}\text{Cu}_{0.25}\text{Ti}_{0.75}\text{O}_4$, where Ln is (1) La, (2) Pr, and (3) Nd.

anisotropy of the BO_6 coordination polyhedron and the dielectric constant ϵ , and, consequently, a decrease in the anisotropy of AO_9 and $\text{tg } \delta$. To analyze the effects of compression/elongation of the cation–oxygen bonds, the values of normalized bond lengths (the ratios of the calculated metal–oxygen bond lengths to the ionic radii sum of oxygen and metal) in appropriate oxygen coordination can be used. If this ratio is more than 1, then the cation–oxygen bond is elongated, otherwise it is compressed. Figure 4 shows the normalized bond lengths in the coordination polyhedra BO_6 and AO_9 for samples $\text{Ln}_{1-x}\text{Sr}_{1+x}\text{Cu}_{x/2}\text{Ti}_{1-x/2}\text{O}_4$ ($x = 0.5$; Ln = La, Pr, Nd) vs. the tolerance factor t calculated as $r_A + r_O/[2(r_B + r_O)]^{1/2}$. Comparison of the obtained Ln–O distances in the LnO_9 coordination polyhedra shows that the smallest compression of the bond La–O(2b) correlating with the $\text{tg } \delta$ value occurs in oxides, where Ln is La. The $(\text{Cu,Ti})\text{O}_6$ octahedra are most extended in compound $\text{Pr}_{0.5}\text{Sr}_{1.5}\text{Cu}_{0.25}\text{Ti}_{0.75}\text{O}_4$, which exhibits higher ϵ values.

Thus, both ‘external’ (such as the appearance of the Maxwell–Wagner effect in the region of grain boundaries, which is affected

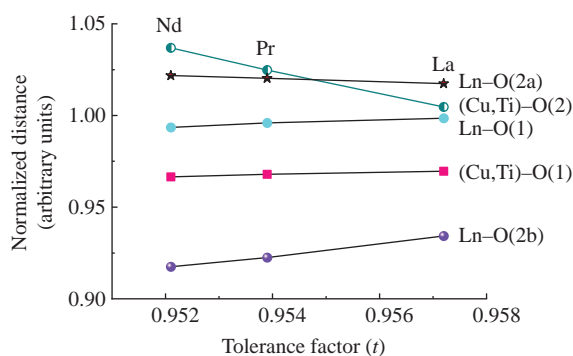


Figure 4 The normalized bond lengths in the coordination polyhedra of oxides $\text{Ln}_{1-x}\text{Sr}_{1+x}\text{Cu}_{x/2}\text{Ti}_{1-x/2}\text{O}_4$ ($x = 0.5$; Ln = La, Pr, Nd).

by gas density and grain size) and ‘internal’ (associated with characteristics of the crystal structure parameters and charge polarization) reasons are responsible for the higher dielectric constant values. From our point of view, the contribution of ‘external’ factors to the dielectric constant value mainly appears at low frequencies, since a significant difference in morphology leads to a noticeable change in the magnitude of the dielectric constant in the frequency domain of 10–1000 Hz [see Figure 3(a)]. ‘Internal’ factors affect the dielectric constant mostly at high frequencies (corresponding to the short times), where the main role is played by intragranular processes associated with the features of polarization relaxation of carriers, which is consistent with the assumed nature of the high dielectric constant of materials possessing the K_2NiF_4 structure.^{1,2}

In conclusion, we have herein reported the data on the synthesis, structure, and dielectric properties of new layered perovskite-like oxides $\text{Ln}_{0.5}\text{Sr}_{1.5}\text{Cu}_{0.25}\text{Ti}_{0.75}\text{O}_4$ (Ln = La, Pr, and Nd) belonging to the structural type of K_2NiF_4 . The low values of dielectric constant ϵ in the range of 20–100 are apparently due to the insufficient anisotropy of coordination polyhedra in the obtained compounds. A lower dielectric loss tangent was observed as compared to other compounds of this structure. The extrapolation of $\text{tg } \delta$ vs. f (Hz) in the interval of high frequencies suggested a further decrease in dielectric losses and a potential of the obtained compounds as materials (e.g., those with a high quality factor Q in the gigahertz range) for practical applications in electronic devices. In addition, it is possible to improve the dielectric characteristics of the considered oxides *via* optimizations of their microstructure.

This work was supported by the Russian Foundation for Basic Research (grant no. 16-02-00857-a) and carried out within the framework of the State Assignment to the Institute of Solid State Chemistry of the Ural Branch of the Russian Academy of Sciences (project no. AAAA-A16-116122810209-5).

References

- 1 K. Meeporn, N. Chanlek and P. Thongbai, *RSC Adv.*, 2016, **6**, 91377.
- 2 P. Lunkenheimer, M. Resch, A. Loidl and Y. Hidaka, *Phys. Rev. Lett.*, 1992, **69**, 498.
- 3 C. H. Chen, S.-W. Cheong and A. S. Cooper, *Phys. Rev. Lett.*, 1993, **71**, 2461.
- 4 S. Krohns, P. Lunkenheimer, Ch. Kant, A. V. Pronin, H. B. Brom, A. A. Nugroho, M. Diantoro and A. Loidl, *Appl. Phys. Lett.*, 2009, **94**, 122903.
- 5 C. C. Homes, T. Vogt, S. M. Shapiro, S. Wakimoto and A. P. Ramirez, *Science*, 2001, **293**, 673.
- 6 C. Stuedtner, E. Morán, M. Á. Alario-Franco and J. L. Martínez, *J. Mater. Chem.*, 1997, **7**, 661.
- 7 C.-Y. Shi, Z.-B. Hu and Y.-M. Hao, *J. Alloys Compd.*, 2011, **509**, 1333.
- 8 X.-C. Fan, X.-M. Chen and X.-Q. Liu, *Chem. Mater.*, 2008, **20**, 4092.

Received: 4th October 2018; Com. 18/5710